Biochimica et Biophysica Acta 1828 (2013) 1899–1908

Contents lists available at SciVerse ScienceDirect

Biochimica et Biophysica Acta

journal homepage: www.elsevier.com/locate/bbamem

A biophysical approach to menadione membrane interactions: Relevance for menadione-induced mitochondria dysfunction and related deleterious/therapeutic effects

João P. Monteiro [a,b], André F. Martins [a,b], Cláudia Nunes [c], Catarina M. Morais [a,b], Marlene Lúcio [c], Salette Reis [c], Teresa J.T. Pinheiro [d], Carlos F.G.C. Geraldes [a,b], Paulo J. Oliveira [a], Amália S. Jurado [a,b,*]

[a] CNC — Center for Neuroscience and Cell Biology, University of Coimbra, Portugal
[b] Department of Life Sciences, University of Coimbra, Portugal
[c] REQUIMTE, Departamento de Química, Faculdade de Farmácia, Universidade do Porto, Portugal
[d] School of Life Sciences, University of Warwick, Coventry, United Kingdom

ARTICLE INFO

Article history:
Received 9 August 2012
Received in revised form 20 March 2013
Accepted 8 April 2013
Available online 13 April 2013

Keywords:
Lamellar and inverted hexagonal phases
Lateral phase separation
Membrane fluidity and permeability
Membrane models
Menadione
Mitochondria

ABSTRACT

Menadione (MEN), a polycyclic aromatic ketone, was shown to promote cell injury by imposing massive oxidative stress and has been proposed as a promising chemotherapeutic agent for the treatment of cancer diseases. The mechanisms underlying MEN-induced mitochondrial dysfunction and cell death are not yet fully understood. In this work, a systematic study was performed to unveil the effects of MEN on membrane lipid organization, using models mimicking mitochondrial membranes and native mitochondrial membranes. MEN was found to readily incorporate in membrane systems composed of a single phospholipid (phosphatidylcholine) or the lipids dioleoylphosphatidylcholine, dioleoylphosphatidylethanolamine and tetraoleoylcardiolipin at 1:1:1 molar ratio, as well as in mitochondrial membranes. Increased permeability in both membrane models, monitored by calcein release, seemed to correlate with the extent of MEN incorporation into membranes. MEN perturbed the physical properties of vesicles composed of dipalmitoylphosphatidylcholine or dipalmitoylphosphatidylethanolamine plus tetraoleoylcardiolipin (at 7:3 molar ratio), as reflected by the downshift of the lipid phase transition temperature and the emergence of a new transition peak in the mixed lipid system, detected by DSC. ^{31}P NMR studies revealed that MEN favored the formation of non-lamellar structures. Also, quenching studies with the fluorescent probes DPH and TMA-DPH showed that MEN distributed across the bilayer thickness in both model and native mitochondrial membranes. MEN's ability to promote alterations of membrane lipid organization was related with its reported mitochondrial toxicity and promotion of apoptosis, predictably involved in its anti-carcinogenic activity.

1. Introduction

Menadione (2-methyl-1,4-naphthoquinone or vitamin K_3; MEN) is a polycyclic aromatic ketone (Fig. 1) that can function as a precursor in the synthesis of vitamin K. MEN reduction at the level of the complex I of the mitochondrial respiratory chain [1,2], which accounts for 50% of its metabolism [2], readily diverts the electron flow from the normal flux to complex II. As a quinone, MEN may undergo one-el2ectron reduction producing a semiquinone radical, which in turn reduces molecular oxygen into superoxide anion radical, while being oxidized back to the initial quinone form [3]. This futile redox cycling generating intracellular ROS may elicit rapid oxidation of biological molecules in both the mitochondrial matrix and cytosol, thus justifying the common use of MEN as a model compound to investigate the mechanisms of oxidative stress and apoptosis [3].

MEN pharmacological importance as a chemotherapeutic agent in cancer diseases [4], such as leukemia [5,6], gastrointestinal [7] and lung [8] cancers, has been reported. Positive outcomes of the administration of MEN on pancreatic [9] and prostate cancer, in this case in association with vitamin C [10], have been recognized too. However, the exposure to MEN has also been associated with several adverse effects, including hemolytic anemia [11,12], cardiotoxicity [13], hepatotoxicity [14] and neuronal damage [15].

Abbreviations: $\Delta\Psi$, mitochondrial transmembrane potential; cyt c, cytochrome c; DMF, dimethylformamide; DOPC, dioleoylphosphatidylcholine; DOPE, dioleoylphosphatidylethanolamine; DPH, 1,6-diphenyl-1,3,5-hexatriene; TMA-DPH, trimethylammonium-diphenylhexatriene; DPPC, dipalmitoylphosphatidylcholine; DPPE, dipalmitoylphosphatidylethanolamine; DSC, differential scanning calorimetry; FCCP, carbonylcyanide p-trifluoromethoxyphenylhydrazone; IMM, inner mitochondrial membrane; MEN, menadione; MPT, mitochondrial permeability transition; NBD-PE, L-α-Phosphatidylethanolamine-N-(4-nitrobenzo-2-oxa-1,3-diazole); ^{31}P NMR, phosphorous nuclear magnetic resonance; POPC, palmitoyloleoylphosphatidylcholine; ROS, reactive oxygen species; TOCL, tetraoleoylcardiolipin

* Corresponding author at: Center for Neurosciences and Cell Biology, University of Coimbra, Largo Marquês de Pombal, 3004-517 Coimbra, Portugal. Tel.: +351 239 853600; fax: +351 239 855789.
E-mail address: asjurado@bioq.uc.pt (A.S. Jurado).

0005-2736/$ – see front matter © 2013 Elsevier B.V. All rights reserved.
http://dx.doi.org/10.1016/j.bbamem.2013.04.006

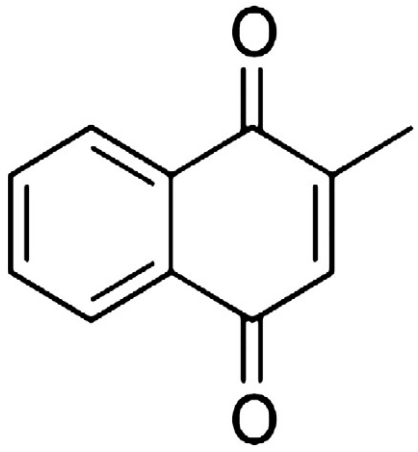

Fig. 1. Chemical structure of menadione (2-methyl-1,4-naphthoquinone).

Given their lipophilic character, MEN molecules hold a predictably high proneness to incorporate into membrane environments. Studies performed in our laboratories have shown that many lipophilic compounds, such as clinically-used drugs [16–19] and environmental pollutants, including insecticides [20–23] and organotins [24], promote alterations of membrane physical properties, with repercussions in membrane-associated functions, including those related to mitochondrial bioenergetics. Consistently, MEN membrane incorporation has been reported to enhance membrane fluidity, this mechanism having been proposed to mediate MEN toxicity in rat hepatocytes [25]. On the other hand, MEN was found to affect mitochondrial respiration, as reflected by changes in several respiratory parameters, namely an increase in respiratory state 4 and a decrease in the respiratory control index and ADP/O ratio [26]. MEN-induced increase in state 4 respiration has been assigned to increased basal permeability of the inner mitochondrial membrane (IMM) to protons, which may result from membrane physical perturbations.

Fluidity is a critical property of membranes that interferes with the activity of membrane proteins [27] and modulates membrane permeability [28]. However, the full picture of drug-membrane interactions and their functional repercussions may involve further characterization of membrane physical properties, such as curvature stress associated to the lipid propensity to form non-lamellar-phases. This type of lipid assemblies has been proposed to play a role in cell fusion and fission processes [29] and in the recruitment of proteins involved in signal amplification [30,31]. Hexagonal II structures (H_{II}) have been proposed to be present at membrane contact sites such as those between the inner and outer mitochondrial membranes, where the mitochondrial permeability transition (MPT) pore is thought to be formed [32]. MPT was suggested as being essential for MEN-elicited apoptosis, promoting efflux of cytochrome *c* (cyt *c*) into the cytoplasm and subsequent activation of caspases 9 and 3 [33]. Although it has been reported that MEN induced MPT [34] by a process involving direct oxidation of mitochondrial pyridine nucleotides and modification of critical thiols of MPT pore components [35], other mechanisms may underlie MEN effects on this process.

Attempting to approach membrane physical effects exerted by MEN, which could be associated with the impairment of mitochondria functioning and apoptosis, biophysical studies were carried out in the present work employing diverse techniques and a variety of membrane preparations. These included membrane models mimicking the cardiolipin-enriched IMM (where most mitochondrial proteins lie), namely at the contact sites between inner and outer mitochondrial membranes (where MPT pore is formed), and native mitochondrial membranes.

These studies provided evidence that MEN affected membrane physical properties, which could be critical for membrane protein activity and susceptible of compromising important mitochondria-driven physiological processes, including cell death, hence unveiling novel targets for MEN to exert its action either therapeutic or detrimental.

2. Materials and methods

2.1. Chemicals

The lipids dipalmitoylphosphatidylcholine (DPPC), palmitoyloleoylphosphatidylcholine (POPC), dioleoylphosphatidylcholine (DOPC), dipalmitoylphosphatidylethanolamine (DPPE), dioleoylphosphatidylethanolamine (DOPE), tetraoleoylcardiolipin (TOCL) (at least 98% pure) and the fluorescent lipid probe L-α-Phosphatidylethanolamine-N-(4-nitrobenzo-2-oxa-1,3-diazole) (NBD-PE) were obtained from Avanti Polar Lipids, Inc. (Murcia, Spain). MEN was purchased from Sigma Chemical Co. (St. Louis, MO, USA). The probes calcein, 1,6-diphenyl-1,3,5-hexatriene (DPH) and trimethylammonium-diphenylhexatriene (TMA-DPH) were purchased from Molecular Probes, Inc. (Eugene, OR, USA). All the other chemicals were of the highest commercially available purity.

2.2. Preparation of multilamellar vesicles (MLVs)

Adequate portions of DPPC or mixtures of DPPE:TOCL (7:3 molar ratio) and DOPC:DOPE:TOCL (1:1:1 molar ratio) were dissolved in chloroform, and subsequently evaporated to dryness in a rotary evaporator. The dry residues were hydrated under N_2 atmosphere by gentle shaking with an adequate volume of buffer (10 mM Tris-maleate plus 50 mM KCl, pH 7.0, for DPPC and DPPE:TOCL liposomes and 50 mM HEPES plus 0.2 mM NaCl, pH 7.5, for DOPC:DOPE:TOCL liposomes) at a temperature above the transition phase of the respective lipid preparations (room temperature for the ternary unsaturated lipid mixture, 55 °C for DPPC and 65 °C for DPPE:TOCL mixture). DPPC and DPPE:TOCL preparations (150 mM in lipid), used in DSC assays, and DOPC:DOPE:TOCL preparations (5 mg), used in ^{31}P NMR assays were vortexed three times during 1 min to disperse aggregates. MEN was then added to the liposome suspensions from a concentrated ethanolic solution, and the preparations were allowed to equilibrate overnight at the temperatures at which liposomes were prepared (i.e. at temperatures above T_m). Control samples were prepared with equivalent volumes of ethanol, which were always less than 3% of the total volume of the sample. Negligible effects were exerted by these amounts of ethanol (<3% v/v) on the studied membrane systems as detected by the different techniques.

2.3. Preparation of large unilamellar vesicles (LUVs)

For the spectrophotometric and spectrofluorimetric measurements, LUVs were prepared from the corresponding MLV suspensions. Therefore, adequate portions of lipid (POPC, DPPC or a mixture of DOPC:DOPE:TOCL at 1:1:1 molar ratio) were dissolved in chloroform, and MLVs were prepared in buffer (50 mM HEPES plus 0.2 mM NaCl, pH 7.5 for POPC and DOPC:DOPE:TOCL liposomes and 10 mM Tris-maleate plus 50 mM KCl, pH 7.0, for DPPC liposomes) as previously described, at the concentration of 5 mM for binding studies, 40 mM for calcein release assays and 1.8 mM for fluorescence quenching and derivative spectrophotometry assays. For binding assays, NBD-PE in chloroform was mixed with lipids, before drying and hydration, in order to obtain a concentration of 1 mol% in MLVs. For calcein release measurements, a buffer containing 30 mM calcein was used for the hydration of lipids and MLVs were submitted to several freeze/thaw cycles. MLV suspensions were then extruded 10 times through 100 nm nucleopore polycarbonate filters (Whatman Millipore, USA) to obtain LUV suspensions. In the case of calcein release studies, a molecular exclusion chromatography was subsequently performed to exclude the excess of free probe.

2.4. Preparation of mitochondrial membranes

Mitochondrial membranes prepared from isolated mitochondria [36] and resealed after 5 freeze/thaw cycles in liquid nitrogen were kept at 4 °C, in a buffer (10 mM Tris-maleate, 50 mM KCl; pH 8.5) to which the protease inhibitor phenylmethylsulfonyl fluoride (PMSF, 10 μM) was added. The protein content was determined by the biuret method [37]. Samples containing 2.48 mg of protein/mL (corresponding to a lipid concentration of approximately 400 μM [38]) were used in fluorescence quenching studies.

2.5. Incorporation of the probes DPH and TMA-DPH

A small volume of the fluorescent probe (DPH or TMA-DPH) solution in dimethylformamide (DMF) was injected into 345 μM LUV suspensions to obtain a probe:lipid molar ratio of 1:300. LUVs were incubated overnight in the dark, before the incorporation of MEN. In the case of mitochondrial membrane suspensions, fluorescent probes were added to attain a probe:lipid molar ratio of 1:200 and the preparations were incubated at least for 1 h. Control samples were prepared with equivalent volumes of probe solvent (DMF), which were always less than 3% of the total volume of the sample and showed to have no effect on experimental measurements.

2.6. Spectrophotometric measurements

The partition coefficient (K_p) of MEN between membranes and aqueous buffered solutions was assessed using derivative spectrophotometry, without physical phase separation. Buffered solutions of MEN were added to unilamellar vesicles composed of DPPC or DOPC:DOPE:TOCL (1:1:1 molar ratio) or to mitochondrial membranes, in order to obtain a fixed concentration of drug (34 μM) and increasing concentrations of lipids (100–1000 μM). Reference lipid suspensions were prepared in the absence of drug. The absorption spectra of lipid suspensions containing or not MEN were recorded in the 220–520 nm range, at 50 °C for DPPC liposomes; 25 and 70 °C for the mixture DOPC:DOPE:TOCL and 25, 37 and 50 °C for mitochondrial membranes, in a multidetection microplate reader (Synergy HT; Bio-Tek Instruments), accordingly to a well established protocol [39]. Due to temperature control requirement at high temperature (70 °C), the K_p of MEN in the mixture DOPC:DOPE:TOCL was performed in a conventional spectrophotometer (JASCO V-660). The mathematical treatment of the results was performed using a developed routine, K_p Calculator [39]. This routine allows to i) subtract each reference spectrum from the corresponding sample spectrum to obtain corrected absorption spectra, ii) determine the second and third derivative spectra in order to eliminate the spectral interferences due to light scattered by the lipid vesicles and to enhance the ability to detect minor spectral features and to improve the resolution of bands, and iii) calculate the K_p values (M^{-1}) by a nonlinear fitting method.

2.7. Spectrofluorimetric measurements

2.7.1. Binding studies

The extent of the interaction of MEN with membrane models (80 μM in lipid) was evaluated by monitoring the fluorescence of the incorporated lipid probe NBD-PE in the wavelength range of 490 to 650 nm, following excitation at 465 nm, using a Perkin-Elmer LS 55 Luminescence Spectrometer. The values obtained at the emission peak (528 nm) for each MEN concentration were subtracted from the intensity of fluorescence of a control sample without MEN (but containing a volume of ethanol corresponding to the maximum amount of MEN solution assayed). The differences between the fluorescence intensities were expressed as percentages of the total fluorescence of the control and then plotted as a function of MEN to lipid molar ratio.

2.7.2. Calcein release studies

Unilamellar vesicles (100 μM in lipid) containing entrapped calcein were incubated with MEN for 10 min at room temperature. The extent of calcein release was determined by monitoring the fluorescence in the wavelength range from 495 to 580 nm, following excitation at 490 nm, using a Perkin-Elmer LS 55 Luminescence Spectrometer. The values obtained at the emission peak (510 nm) were normalized to the total amount of calcein released after disruption of vesicles with 0.1% Triton X-100 and plotted as a function of MEN to lipid molar ratio.

The percentage of calcein release induced by X concentration of the compound, reflecting the permeability of vesicle membranes (% P*x*), was calculated using the following formula:

$$\%Px = \frac{I_X - I_C}{I_T} \cdot 100 \quad (1)$$

where, I_X is the fluorescence intensity with *X* concentration of the compound, I_C is the control fluorescence intensity and I_T is the maximal fluorescence intensity after lysis by Triton X-100. Ethanol (an amount equivalent to that of MEN solution added to the samples) had no significant effect on calcein release.

2.7.3. Fluorescence quenching

Fluorescence quenching assays in unilamellar vesicles or mitochondrial membranes containing DPH or TMA-DPH and MEN or ethanol (control) were performed in a Perkin-Elmer LS 55 Luminescence Spectrometer at controlled temperatures (50 °C for DPPC liposomes; 25 and 70 °C for the mixture DOPC:DOPE:TOCL and 25, 37 and 50 °C for the mitochondrial membranes). Excitation wavelength was set at 357 and 361 nm for acquisition of emission spectra of DPH and TMA-DPH, respectively, and the emission wavelength was set at 427 nm for excitation spectra acquisition for both probes. Fluorescence values were corrected for light scattering contributions by subtracting the intensities from unlabeled samples at the same conditions: such contributions were always negligible (less than 0.5%). All fluorescence intensity data were corrected from reabsorbtion and inner filter effects [40].

Fluorescence lifetime measurements were made with a Fluorolog Tau-3 Lifetime system. Modulation frequencies were acquired between 5 and 110 MHz. Integration time was 8 s. Manual slits used were 1.0 mm, slits for excitation monochromator were 7.000 (side entrance) and 0.5 mm (side exit) and for emission monochromator 7.000 (side entrance) and 7.000 (side exit). All measurements were made using Ludox as a reference standard ($\tau = 0.00$ ns).

2.8. Differential scanning calorimetry

Multilamellar vesicles (150 mM in phospholipid) prepared as described above, containing different amounts of MEN in order to obtain drug:lipid molar ratios from 1:6 to 1:48, or ethanol (control), were sealed into aluminum pans and heating scans were performed over an appropriate temperature range, on a Perkin-Elmer Pyris 1 differential scanning calorimeter at a scan rate of 5 °C/min. To check data reproducibility, three heating scans were recorded for each sample. To compensate the effect of high heat capacity of the aqueous medium on the baseline, an estimated amount of buffer was used in the reference pan. Data acquisition and analysis were performed using the software provided by Perkin Elmer. Distinct temperatures were automatically defined for each endotherm: the onset temperature (T_0) and the temperature at the endotherm peak (T_m). To define the range of the phase transition or lateral phase separation (T_f–T_0), a third temperature was determined (T_f) by extrapolating to the baseline a tangent to the descendent slope of the endothermic peak. These critical transition temperatures were estimated as the mean value of three heating scans in at least three different samples from the same preparation. To determine the total amount of phospholipid

contained in each pan, the pans were carefully opened at the end of the experiment and the content was dissolved in chloroform plus methanol. The phospholipid content was determined by measuring the amount of inorganic phosphate [41], after hydrolysis of the extracts in 70% HClO4, at 180 °C, for 60 min [42]. Finally, peak profiles and enthalpy (ΔH) values were normalized to the exact phospholipid content in each pan.

2.9. ^{31}P NMR

For ^{31}P NMR studies, preparations containing 5 mg of a mixture of DOPC:DOPE:TOCL (1:1:1) were obtained as described above. MEN was added to the liposome suspensions from a concentrated ethanolic solution and the preparations were allowed to stabilize overnight. The samples were loaded into a 5-mm diameter NMR tube and a small volume of a $CaCl_2$ solution was added to reach 1:1 Ca^{2+}:cardiolipin molar ratio. Controls were prepared with a few μl of ethanol, corresponding to the volume of the MEN solution assayed. Spectra were obtained using a Varian Unity 500 NMR spectrometer operating at 202.33 MHz with a 5-mm broadband probe over a 30-kHz sweep width with 60 × 1024 data points. A 90° pulse width of 14.09 μs was used. Composite pulse decoupling allowed to remove any proton coupling. Generally, 800 free induction decays were acquired and processed using an exponential line broadening of 100 Hz prior to Fourier transformation. Probe temperature was maintained to ±0.2 °C by the variable temperature unit of the NMR spectrometer.

2.10. Statistical analysis of data

DSC and fluorescence data, namely transition temperature midpoints (T_m), transition temperature ranges (T_f–T_0), enthalpy changes (ΔH) and quenching percentages were expressed as means ± standard deviation of 3–4 independent experiments. Multiple comparisons were performed using one-way ANOVA with the Student–Newman–Keuls as a post-test. A value of $P < 0.05$ was considered statistically significant.

3. Results

3.1. Menadione binding to membrane model systems depends on lipid composition

The interaction of increasing concentrations of MEN with NBD-PE-containing unilamellar vesicles composed of POPC (electrically neutral) or DOPC:DOPE:TOCL at 1:1:1 molar ratio (negatively charged) induced a progressive decrease of the fluorescence intensity of the lipid probe. This effect, which can be assigned to binding or incorporation of the drug to/into NBD-PE-containing lipid bilayers, results from the high sensitivity of the fluorescent probe to the dielectric constant of its environment [43]. As expected, data obtained with both membrane systems pointed to a saturation type dynamics, indicating that MEN incorporation attained a limit at certain concentrations, which were much higher in POPC than in DOPC:DOPE:TOCL vesicles. In fact, the maximal difference between the fluorescence intensities at the peak of emission in the presence and in the absence of MEN was twofold in the former vesicles as compared to the latter (Fig. 2A). This means that MEN bound/incorporated more strongly to the neutral bilayers than to those displaying a negative charge.

3.2. Menadione increases membrane permeability to calcein

The effects of MEN on membrane permeability were addressed by using the fluorescent probe calcein, encapsulated in unilamellar vesicles with the same composition of those assayed for binding. The concentration at which calcein was encapsulated in vesicles promoted self-quenching of the probe. Therefore, membrane destabilization accompanied by calcein release was assessed by an increase of the fluorescence intensity, as self-quenching decreased. As shown in Fig. 2B, MEN increased the permeability of both membrane systems assayed, but the membrane disturbance induced by MEN was stronger for POPC vesicles than for the lipid mixture. This is consistent with the higher binding or incorporation of the drug observed in the former vesicles (Fig. 2A), indicating that increased incorporation led, as expected, to more drastic effects on membrane permeability.

3.3. Menadione exhibits high partition coefficients in membrane model systems and mitochondrial membranes

The determination of MEN partition coefficients (K_p) by UV–VIS derivative spectrophotometry was based on the change of spectral characteristics of the drug when it left the aqueous solution and incorporated into the lipid phase. The derivative spectra of MEN incorporated in LUVs or mitochondrial membranes exhibited a bathochromic shift in λ_{min} (i.e. the λ at which a selected peak of the derivative spectrum attained a minimum value) up to 2 nm as the lipid concentration increased. This observation provided a clear indication that the drug partitions from the aqueous to the lipid media [39]. MEN K_p values for all the systems studied (Table 1) were obtained by a nonlinear least-squares regression method (Fig. 3) at wavelengths at which the light scattering was very low. The partition of MEN in vesicles composed of DOPC:DOPE:TOCL was not assessed at 70 °C, due to the formation of tatters in the vesicle suspension, which interfered with absorbance measurements, promoting high light scattering.

The incorporation of MEN into membranes showed to be deeply dependent on membrane composition and temperature (Table 1). The higher MEN partition in DPPC vesicles as compared to vesicles composed of a lipid mixture showed a significant parallelism with the higher binding of MEN (assessed by the NBD-PE assay) and the higher MEN-induced membrane permeabilization (evaluated by calcein release) observed for the former membranes relative to the latter. Taking into account that both membranes are in the fluid phase at the temperatures of the assays (50 °C for DPPC vesicles and 25 °C for vesicles of the lipid mixture), their different abilities to incorporate MEN should be assigned to the charge of phospholipid components, negatively charged membranes offering a less favorable medium for MEN incorporation. Since cardiolipin is an anionic phospholipid existing in a significant amount in mitochondrial membranes, partition values in these membranes similar to those obtained in the mitochondrial membrane-mimicking model would be expected. The higher partition of MEN in the native membranes should result from a high affinity of MEN for membrane proteins or from an extra incorporation of the drug through the lipid-protein boundaries. On the other hand, the increase of MEN partition in the fluid mitochondrial membranes at increasing temperatures should reflect a decrease of lipid packing, favoring MEN penetration within the lipid bilayer.

3.4. Menadione affects the thermotropic behavior of membrane lipid models

DSC studies were performed to investigate the effects of MEN on the membrane biophysical properties of two membrane models: DPPC liposomes, as a classical model system for biophysical studies, and a mixed lipid system containing DPPE plus TOCL (representing two important lipid classes of the IMM). DSC thermograms of DPPC bilayers showed, as expected two typical endotherms (Fig. 4A), corresponding to the pre-transition at 35.6 °C, with a low enthalpy change, and the main transition, from a gel to a liquid-crystalline phase, detected as a sharp peak centered at 42.4 °C with an enthalpy change of 38.5 J/g (Table 2). MEN abolished the pre-transition peak (Fig. 4A), even at the lowest concentration assayed (MEN:DPPC molar ratio of 1:48), and increasing concentrations of MEN induced a shift of the main transition temperature towards progressively lower temperatures; the highest MEN concentration assayed promoted a decrease

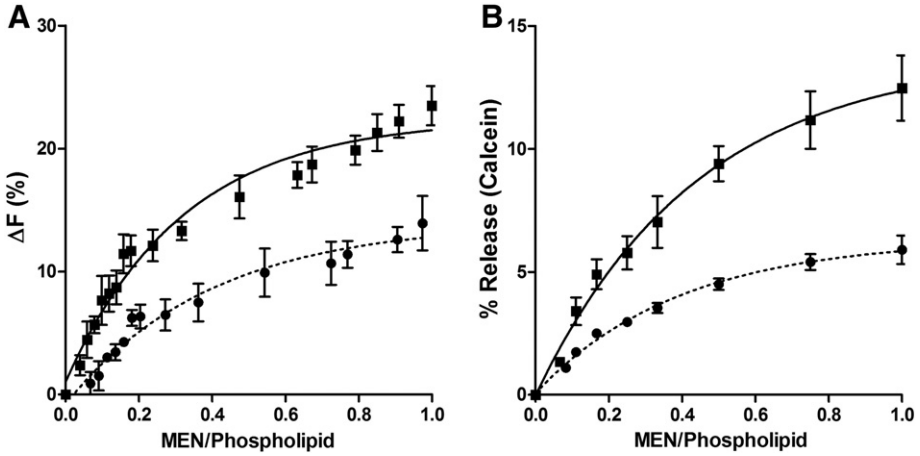

Fig. 2. Interaction of MEN with unilamellar vesicles composed of POPC (squares, full line), or DOPC:DOPE:TOCL (1:1:1) mixture (circles, dashed line), as monitored by NBD-PE (A) and calcein release (B). In the binding studies (A), the extent of MEN incorporation into the membrane models was evaluated as the differences between the fluorescence intensity (ΔF) of NBD-PE incorporated in a control sample (containing a volume of ethanol corresponding to the maximum amount of MEN solution assayed) and in samples containing different MEN:lipid molar ratios, expressed as percentages of the total fluorescence of the control, at 528 nm (corresponding to the peak of NBD-PE emission spectrum). In the calcein release studies (B), data are presented as differences between the fluorescence intensity of calcein, at 510 nm, in MEN-containing and control preparations, normalized as percentages of the maximal fluorescence intensity corresponding to the total (100%) release of calcein, induced by Triton X-100.

of T_m of about 3.1 °C (Table 2). MEN also promoted a progressive broadening of DPPC main transition, reflecting a decrease of the cooperativity, and an increase of the enthalpy (Table 2).

Liposomes prepared from DPPE and TOCL at a molar ratio of 7:3 showed a single, but broad (T_f–$T_0 \approx 10$ °C) endotherm centered at about 48.2 °C (Fig. 4B and Table 2). This behavior was expected taking into account that the lipid components of this mixture hold, when isolated, a large gap between their transition temperatures (64 °C for DPPE and below 0 °C for TOCL) as previously reported [44]. This mixture is prone to undergo lateral phase separation. The addition of MEN to these liposomes promoted the emergence of a new endothermic peak with a higher transition temperature than that of the control lipid preparation (without drug), suggesting the formation of DPPE-enriched lipid domains. Regarding the enthalpies of the transitions (ΔH), the sum of the enthalpies corresponding to the two endotherms exhibited by MEN-containing lipid preparations was approximately equivalent to the enthalpy of the control preparation, confirming the occurrence of a lateral phase separation (Table 2). On the other hand, the enthalpy of the second peak significantly increased as the concentration of MEN increased (from 1:12 to 1:6 MEN:lipid molar ratio), reflecting an enlargement of the segregated DPPE-enriched domains (Table 2). Interestingly, this peak was also shifted to lower temperatures as MEN concentration increased.

3.5. Menadione changes the membrane phase equilibrium in mixed non-bilayer and bilayer lipid systems favoring the hexagonal II phase

The effect of MEN on lipid mesomorphism exhibited by a ternary lipid system containing bilayer (DOPC) and non-bilayer prone phospholipids (DOPE and TOCL plus calcium) was investigated by ^{31}P NMR. This mixture mimicked the IMM, since it contained the three major components of that membrane. The mixture of DOPC:DOPE:TOCL:Ca^{2+} (1:1:1:1 molar ratio) at 25 °C is mainly organized in extended bilayers (giving rise to the characteristic asymmetrical ^{31}P NMR lineshape with a low-field shoulder and a high-field peak [45] separated by approximately 10 ppm), but part of the component lipids is organized in an inverted hexagonal phase, as evidenced by the small peak downfield of phosphoric acid (set at 0 ppm) which became more evident in the spectrum as the temperature increased (Fig. 5). At 70 °C, the H_{II} phase notoriously predominated relatively to the bilayer component, an effect likely prompted by the presence of Ca^{2+} which compels CL to form non-lamellar arrangements [46]. The incorporation of MEN (at a molar ratio of 1:6 to lipid) affected lipid phase behavior, the H_{II} phase becoming clearly the predominant component above 25 °C.

3.6. Menadione location within the membrane depended on membrane lipid composition and structure

The preferential location of MEN along the depth of the bilayer was investigated by steady-state and time-resolved fluorescence

Table 1
Partition coefficients of MEN obtained in a biphasic membrane/aqueous system. The partition was determined for vesicles composed of DPPC at 50 °C, a lipid mixture containing DOPC:DOPE:TOCL (1:1:1) at 25 °C and isolated mitochondrial membranes at 25 °C, 37 °C and 50 °C.

Lipid	Temperature (°C)	K_p (M^{-1})
DPPC	50.0 ± 0.1	2299 ± 288
Lipid mixture	25.0 ± 0.1	1603 ± 198
Mitochondrial membranes	25.0 ± 0.1	2823 ± 204
	37.0 ± 0.1	3598 ± 108
	50.0 ± 0.1	7781 ± 407

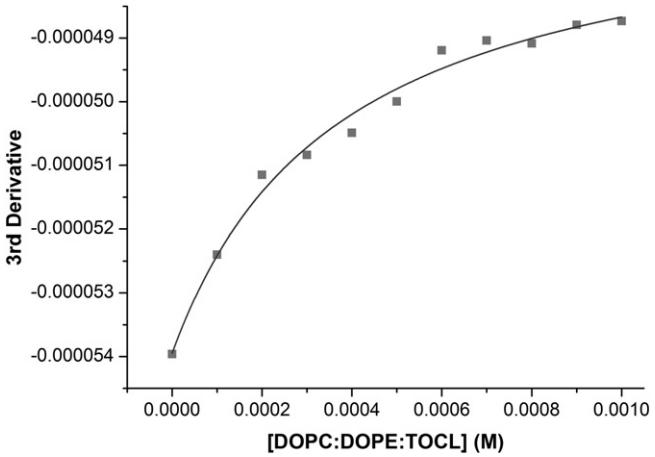

Fig. 3. Fitting curve to experimental third-derivative spectrophotometric data at 298 nm (where the scattering is very low or null) as a function of lipid concentration (LUVs composed of DOPC:DOPE:TOCL at 1:1:1 molar ratio) at 25 °C, using a nonlinear least squares regression method.

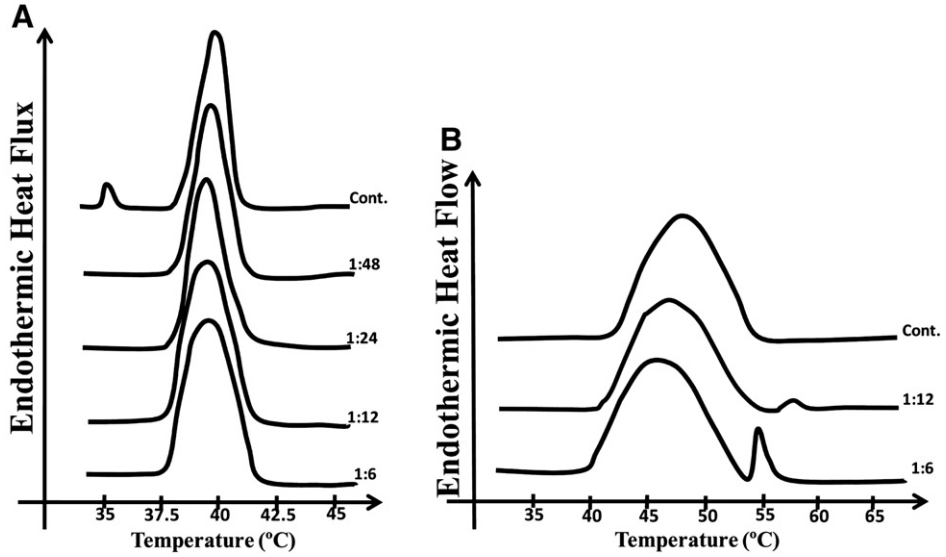

Fig. 4. DSC thermograms of liposomes prepared from DPPC (A) or a mixture of DPPE and TOCL at a 7:3 molar ratio (B), in the absence (cont.) or presence of MEN at the MEN:lipid molar ratios indicated on the scans. The DSC profiles were originated from heating scans. The thermograms are typical assays of at least three independent experiments.

studies using two fluorescent probes: DPH, buried in the hydrocarbon core [47], and TMA-DPH, which due to its charged group anchored at the lipid water interface reports the region of the bilayer corresponding to the upper portions of the lipid hydrocarbon chains [48].

Since only drug molecules distributed in the membrane are able to quench the probes inserted in lipid bilayers, the effective concentrations of MEN within the membrane ($[MEN]_m$) rather than the total concentrations of the drug ($[MEN]_T$) were used in the subsequent fluorescent quenching studies to localize MEN through the membrane thickness. In order to calculate membrane effective concentrations of MEN, K_p values were used in the following equation [40]:

$$[MEN]_m = \frac{K_p[MEN]_T}{K_p\alpha_m + (1-\alpha_m)} \quad (2)$$

where α_m is the volume fraction of membrane phase ($\alpha_m = V_m/V_T$; V_m and V_T representing the volumes of the membrane and water phases, respectively). For vesicles of DOPC:DOPE:TOCL at 70 °C, the $[MEN]_m$ for the same system at 25 °C was used, since the K_p was not determined at the high temperature due to the difficulties previously referred, probably caused by the formation of hexagonal phases as demonstrated by ^{31}P NMR.

In DPPC vesicles, MEN induced a concentration dependent reduction of DPH and TMA-DPH fluorescence (Fig. 6A and B). The extent of fluorescence quenching induced in both probes was evaluated by plotting steady-state fluorescence (F_0/F) and lifetime measurements (τ_0/τ) as a function of MEN concentration (Fig. 6C and D) according to the Stern–Volmer equations [40]:

$$\frac{F_0}{F} = 1 + K_{SV}[MEN] \quad (3)$$

$$\frac{\tau_0}{\tau} = 1 + K_D[MEN] \quad (4)$$

where (F, τ) and (F_0, τ_0) are steady-state fluorescence intensities and lifetimes in the presence and in the absence of MEN, respectively, and K_{SV} and K_D are the Stern–Volmer constants, which indicate the extension of quenching. Whereas K_{SV} reflects the occurrence of both dynamic (collisional) and static (resulting from the formation of a complex

Table 2
Characterization of the phase transitions detected by DSC (temperature of the endothermic peak, T_m, transition temperature range, T_f–T_o, and enthalpy change, ΔH) in liposomes of DPPC or DPPE:TOCL (7:3). Liposomes were incubated with MEN to obtain different drug:lipid molar ratios (indicated in the Table) or with a few μl of ethanol (corresponding to the maximal volume of the MEN solution assayed) for the respective control (MEN:lipid molar ratio of zero in the Table).

MEN:lipid molar ratio	T_m (°C)	T_f–T_0 (°C)	ΔH (J/g)	T_m 2 (°C)	ΔH 2 (J/g)
MEN:DPPC	Peak 1			Peak 2	
0 (control)	42.43 ± 0.4096***	2.25 ± 0.1849	38.54 ± 0.5618	–	–
1:48	41.53 ± 0.2145^{ns}	2.75 ± 0.05462*	39.68 ± 0.3734^{ns}	–	–
1:24	40.74 ± 0.2228*	3.14 ± 0.07364*	41.48 ± 0.7017*	–	–
1:12	40.32 ± 0.2191**	3.56 ± 0.07209**	42.08 ± 0.6974*	–	–
1:6	39.36 ± 0.1759**	4.48 ± 0.3725**	43.16 ± 1.240*	–	–
MEN:lipid mixture					
0 (control)	48.16 ± 2.00	9.45 ± 1.98	20.18 ± 0.77	–	–
1:12	46.79 ± 1.72^{ns}	10.53 ± 1.71*	19.80 ± 0.79*	57.82 ± 0.60	0.41 ± 0.22
1:6	45.19 ± 0.34*	11.07 ± 2.05**	18.11 ± 0.56**	54.62 ± 1.92*	2.79 ± 0.79**

a) Values presented are means ± standard deviation of three to four DSC experiments. Comparisons were performed using one-way ANOVA, with the Student–Newman–Keuls as a post-test for the following paired observations: liposomes with each MEN:lipid molar ratio vs. control liposomes (without MEN). n.s., not significant.
*** $P < 0.001$.
** $P < 0.01$.
* $P < 0.05$.

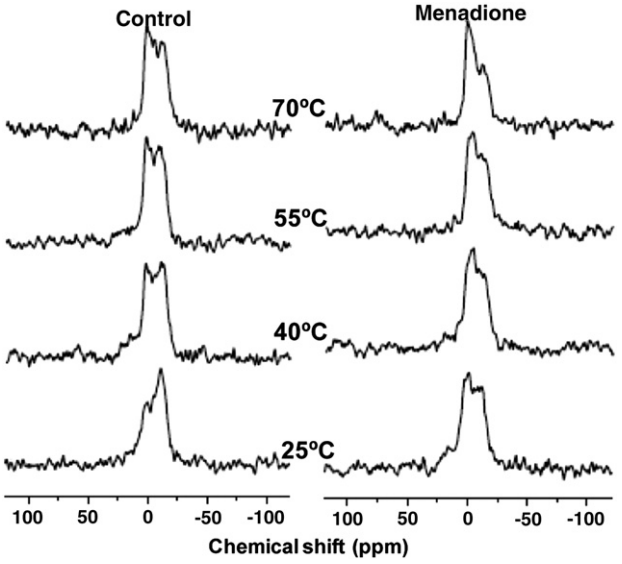

Fig. 5. ^{31}P NMR spectra of aqueous dispersions of DOPC:DOPE:TOCL (1:1:1) with $CaCl_2$ (1:1 to cardiolipin) at different temperatures (indicated in the figure), in the absence (Control) or the presence of MEN at a 1:6 drug to phospholipid molar ratio (Menadione). For each sample, the spectrum was first averaged at 25 °C over a period of about 20 min, and then the process was repeated over a range of temperatures with 15 °C increments. Each sample (600 μl) contained 5 mg of total lipid.

between the probe and the quencher) quenching processes, K_D reflects exclusively a dynamic quenching process.

As shown in Fig. 6C and D, the dynamic quenching represented by the lifetime Stern–Volmer plot (dotted line) was lower than the quenching gathered from steady-state fluorescence measurements (solid line) for both probes, indicating the occurrence of an additional static quenching process, which did not influence excited state lifetimes. Therefore, the quenching process was analyzed by a modified form of the Stern–Volmer equation, which accounts for the additional static quenching [40]:

$$\frac{F_0}{F(1+K_D[MEN])} = (1+K_S[MEN]). \quad (5)$$

This expression contemplates the dynamic quenching component characterized by the dynamic Stern–Volmer constant K_D, as well as the static component, characterized by the static Stern–Volmer constant K_S. The K_D component was experimentally determined as the slope of the lifetime measurement plot. On the other hand, a plot of (F_0/F) / $(1+K_D$ [menadione]) versus [menadione] yielded a straight line with an intercept of 1 and a slope of K_S (data not shown).

The quenching parameters obtained from the analysis of the Stern–Volmer plots (K_D from collisional quenching, K_S from static quenching and K_{SV}, as the sum of both contributions) are shown in Table 3.

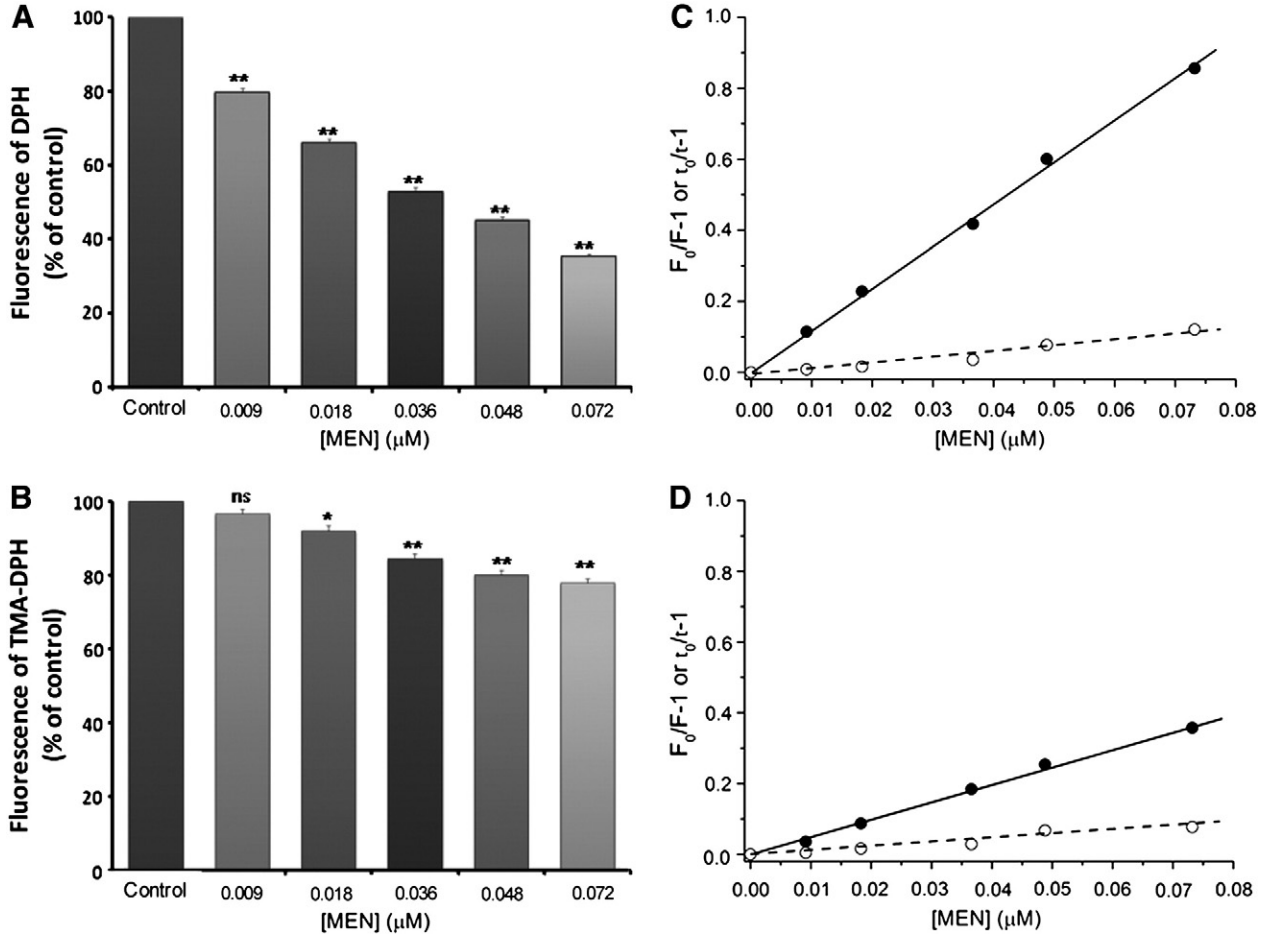

Fig. 6. Quenching effects of MEN on the emission of DPH (A) and TMA-DPH (B) incorporated in DPPC unilamellar vesicles as a function of the effective concentrations of MEN within the membranes, measured at 427 nm. The corresponding Stern–Volmer plots are represented for the probes DPH (C) and TMA-DPH (D) as a function of MEN concentration. Stern–Volmer plots were obtained from steady state fluorescence measurements (black circles) and from fluorescence lifetime measurements (white circles). Lines are the best fit for Eqs. (3) (solid line) and (4) (dotted line). Results are representative of at least three independent determinations for each condition. Comparisons were performed using one-way ANOVA, with the Student–Newman–Keuls as a post-test for the following paired observations: LUVs with a membrane MEN concentration of 0.009, 0.018, 0.036, 0.048 or 0.072 μM vs. control LUVs (without MEN); **, $P < 0.01$; *, $P < 0.05$; ns, not significant.

In order to compare the quenching effects on DPH and TMA-DPH, the bimolecular quenching rate constant ($K_q = K_D/\tau_0$) [40] was calculated. This parameter, also shown in Table 3, reflects the efficiency of quenching, which in the case of the present study depends on the accessibility of MEN molecules to the fluorescent probe, eliminating specificities related with the fluorescence lifetime of the probe (τ_0). The analysis of Table 3 data, showing that the K_q value obtained with TMA-DPH incorporated in vesicles of DPPC was higher than that with DPH, suggests a preference of MEN to locate at the shallow hydrophobic regions of DPPC bilayers.

Aiming at establishing a correlation between MEN membrane interactions and its effects on mitochondria, quenching analyses were extended to other more realistic membrane model composed of a lipid mixture of DOPC:DOPE:TOCL at 1:1:1 molar ratio, and also to suspensions of isolated mitochondrial membranes.

Regarding the lipid mixture model at 25 °C, at which temperature ^{31}P NMR data showed that hexagonal phases already prevailed in the presence of MEN, this compound exhibited a preference to be localized closer to the upper regions of lipid acyl chains, monitored by TMA-DPH. Indeed, in these conditions, the K_q value obtained with TMA-DPH was about 87.5% higher than that with DPH. At 70 °C, when H_{II} lipid arrangement clearly predominated, MEN also showed a preferential localization closer to the upper regions of the fatty acyl chains, since the K_q value obtained with TMA-DPH was twice that obtained with DPH. It is worth mentioning that when the lipid mixture in the presence of MEN adopted predominantly an inverted hexagonal structure (at 70 °C), K_q values for DPH and TMA-DPH were respectively 6.9 and 7.3 times higher than those obtained at 25 °C (Table 3), temperature at which a significant component assigned to the lamellar structure was still detected in the ^{31}P NMR spectrum of the MEN-containing lipid mixture. Although being aware that MEN effective concentration in this lipid system was not determined at 70 °C, it is fair to suggest that the significant increase of the K_q value at this temperature indicates that MEN was more efficiently incorporated in this lipid system when arranged in a H_{II} structure, which may justify its tendency to favor this phase to the detriment of the lamellar phase when both phases coexist, as revealed by ^{31}P NMR data.

In isolated mitochondrial membranes, MEN showed a preferential location in the inner bilayer regions close to DPH, which displayed higher quenching by MEN as compared to TMA-DPH. The nature of the quenching process also differed for the two probes. MEN quenched DPH fluorescence exclusively by a dynamic, collisional process.

In contrast, MEN-induced quenching of TMA-DPH fluorescence involved besides a dynamic process a static one, which resulted from the formation of a non-fluorescent ground-state complex between the probe and MEN. Taking into account TMA-DPH localization in the bilayer, it seems reasonable to propose that MEN bounds electrostatically to the head groups of phospholipids. At the highest temperature assayed, the static quenching component disappeared due to complete dissociation of the weakly bound drug-probe complexes and TMA-DPH quenching became exclusively collisional in nature.

4. Discussion

MEN generates intracellular ROS at multiple cellular sites through futile redox cycling [49]. MEN biological activity has been shown to promote either favorable or deleterious effects on cellular functioning. Low levels of MEN-induced oxidative stress have shown to mimic endogenous oxidant signals that trigger protection against ischemic injury in the heart [50]. In contrast, higher concentrations of MEN were proposed to induce toxic oxidative stress associated with tissue injury, mitochondrial DNA damage, and cell death [51–54], and MEN genotoxicity has been attributed to its ability to damage DNA via ROS generation [55]. On the other hand, therapeutic benefits of MEN have been described in the treatment of several types of cancer [5–8].

MEN's capacity to promote lipid peroxidation, associated with its high propensity to incorporate into membranes due to its lipophilic character [55], has been related to MEN-induced human cancer cell degeneration [56]. MEN incorporation into membranes was demonstrated in the present work using liposomes of different composition and isolated mitochondrial membranes. Concomitant disturbances of membrane physical properties were also detected by different techniques (DSC, ^{31}P NMR), likely related with MEN-induced increase of membrane permeability, as deduced by the calcein release assays (Fig. 2). Noteworthy, curves representing MEN-membrane binding/incorporation and MEN-induced calcein release as function of drug concentration allow foreseeing a relationship between MEN membrane interaction and disturbing effects. The increase of calcein release from lipid vesicles in the presence of MEN might be associated to a decrease of lipid packing, which would favor the generation of small free volumes, hence facilitating calcein diffusion across the lipid bilayer. However, more efficiently than a moderate increase of

Table 3
Values of probe lifetimes (τ_m) and of the Stern–Volmer constant corresponding to the dynamic quenching (K_D), the static quenching (K_S), and the combination of the two types of quenching (K_{SV}), as well as the bimolecular quenching constant (K_q) obtained from measurements of fluorescence quenching of DPH and TMA-DPH at different MEN:lipid ratios, for vesicles composed of DPPC or a lipid mixture of DOPC:DOPE:TOCL (1:1:1) with Ca^{2+} 1:1 to cardiolipin at 25 °C or 70 °C. Quenching studies with isolated mitochondrial membranes were also performed at the temperature range from 25 to 50 °C.

Lipid	Probe	K_D (M^{-1}) (a)	K_S (M^{-1}) (b)	K_{SV} (M^{-1})	$\tau_m X10^{-9}$ (s) (c)	K_q $X10^9$ ($M^{-1}s^{-1}$) (d)
DPPC	DPH	1.6 ± 0.2	6.9 ± 0.2	8.6 ± 0.5	7.45 ± 0.05	0.22 ± 0.2
	TMA-DPH	1.1 ± 0.1*	3.3 ± 0.2**	4.5 ± 0.3**	2.68 ± 0.04	0.4 ± 0.1**
Lipid mixture 25 °C (L_α phase)	DPH	1.41 ± 0.06	1.19 ± 0.04	2.6 ± 0.1	8.70 ± 0.04	0.16 ± 0.1
	TMA-DPH	1.16 ± 0.08*	0.98 ± 0.03*	2.2 ± 0.2*	3.85 ± 0.04	0.3 ± 0.1**
Lipid mixture 70 °C (H_{II} phase)	DPH	6.3 ± 0.1	12.7 ± 0.1	19.0 ± 0.2	5.77 ± 0.08	1.1 ± 0.2
	TMA-DPH	2.4 ± 0.02**	2.1 ± 0.1**	4.6 ± 0.1**	1.09 ± 0.05	2.2 ± 0.2*
Mitochondrial membranes 25 °C	DPH	8.5 ± 0.8	–	8.5 ± 0.8	5.14 ± 0.02	1.6 ± 0.8
	TMA-DPH	1.72 ± 0.02**	2.92 ± 0.04	4.65 ± 0.06**	2.35 ± 0.04	0.73 ± 0.06**
Mitochondrial membranes 37 °C	DPH	8.0 ± 0.8	–	8.0 ± 0.8	5.00 ± 0.06	1.6 ± 0.9
	TMA-DPH	1.4 ± 0.2**	1.1 ± 0.2	2.6 ± 0.4**	2.09 ± 0.02	0.7 ± 0.3**
Mitochondrial membranes 50 °C	DPH	8.0 ± 0.3	–	8.0 ± 0.3	4.66 ± 0.05	1.7 ± 0.3
	TMA-DPH	1.49 ± 0.03**	–	1.49 ± 0.03**	1.77 ± 0.03	0.84 ± 0.06**

(a) K_D values were calculated from the slope of the lifetime linear plots (τ_0/τ versus [MEN]) based on Eq. (4).
(b) K_S values were calculated from the slope of the linear plots (F_0/F) / ($1+K_D$ [Q]) versus [MEN] based on Eq. (5).
(c) τ_m values were calculated by the following expression: $\tau_m = \sum f_i \tau_i$, where f_i is the fractional contribution of component i to the total lifetime.
(d) K_q values were calculated using the K_D values and experimental τ_0 of the probe.
Values presented are mean ± standard deviation of at least three experiments. Comparisons were performed using one-way ANOVA, with the Student–Newman–Keuls as a post-test for the following paired observations: lipid models labelled with TMA-DPH vs. corresponding lipid models labelled with DPH at the same temperature.
** $P < 0.001$.
* $P < 0.05$.

membrane fluidity, the occurrence of lateral membrane separation, with the appearance of discontinuities and defect lines in the interface regions between lipid domains at different phases, has shown to promote an increase of membrane permeability [57]. Consistently, DSC studies carried out in a mixed lipid system (7 DPPE: 3 TOCL) showed that MEN induced the segregation of DPPE-enriched domains (Fig. 4B), revealing its capacity to promote lateral phase separation. On the other hand, an increase of MEN concentration promoted a downshift of the transition temperature of the DPPE-segregated domains (Fig. 4B) as well as of the DPPC liposomes (Fig. 4A), reflecting the disordering effect associated with the incorporation of MEN in lipid bilayers. An uneven distribution of MEN into the membrane is suggested by its preferential interaction with zwitterionic phospholipids: DPPE in the mixture of DPPE:TOCL, as deduced from DSC studies; and DPPC/POPC bilayers rather than the DOPC:DOPE:TOCL negatively charged membranes, as demonstrated by partition, binding and calcein release studies (Fig. 2 and Table 1). Therefore, it is expected that in protein-enriched heterogeneous membranes, such as native mitochondrial membranes, MEN should exert a high perturbation of membrane lipid organization. The higher quenching of DPH as compared with TMA-DPH in these membranes, at all temperatures tested, including the physiologic one (Table 3), indicates a deep location of MEN within the lipid bilayer. On the other hand, ^{31}P NMR studies, using membrane models composed of the three most representative lipid classes of mitochondrial membranes (PC, PE and CL) in the presence of Ca^{2+} (an important cation in mitochondria functioning regulation), showed that MEN induced an increased propensity for non-lamellar phase generation (Fig. 5). Altogether, these effects could result in an increase of the permeability of mitochondrial membranes, which could be on the basis of the reported MEN-induced increase of mitochondrial state 4 respiration (a state of passive respiration relying on proton diffusion across the IMM [26]) and decrease of mitochondrial transmembrane potential ($\Delta\Psi$) [33]. Moreover, the perturbation of membrane physical properties could lead to the opening of pores in the membrane through which not only ions could diffuse, but also small molecules could be released. Consistently, MEN-induced activation of apoptosis has been associated with a decrease of $\Delta\Psi$ and the release of cyt *c* from mitochondria to the cytosol [33]. MPT has also been proposed as being involved in this process, its induction being mediated by ROS generation through MEN redox-cycling mechanism [58]. However, our results showed that other mechanisms should be involved in the process by which MEN induced MPT. Thus, the high MEN propensity to induce lateral phase separation in membrane models containing CL, along with its proneness to promote the formation of non-lamellar phases (Fig. 5) may modulate MEN action in CL-enriched mitochondrial membrane regions like the contact sites between the inner and outer mitochondrial membranes [59], where structures of high curvature have been proposed to be present [32] and MPT pore is thought to be formed [60].

In conclusion, this study provides a significant amount of data showing that MEN holds a remarkable membrane activity, which matches its action as an apoptosis enhancer. Moreover, these data provide new elements for understanding previous results regarding MEN toxic effects on rat hepatocytes [25] or MEN-induced apoptosis mediated by MPT and involving mitochondrial cyt *c* release [33]. Finally, the biophysical approach to MEN cellular effects, namely regarding the induction of mitochondrial-mediated apoptosis, should provide new targets to be addressed by MEN or similar compounds in the treatment of diseases such as cancer, where the induction of apoptosis could constitute a therapeutic strategy.

Acknowledgements

The project was supported by the Portuguese Foundation for Science and Technology and FEDER/COMPETE (research grants Pest-C/SAU/LA0001/2011, PTDC-QUI-QUI-101409-2008 and PTDC/QUI-BIQ/103001/2008). J.P.M., A.F.M. and C.M.M. acknowledge FCT for Ph.D. grants SFRH/BD/37626/2007, SFRH/BD/46370/2008 and SFRH/BD/79077/2011, respectively. C.N. thanks FCT for the Pos-Doc Grant SFRH/BPD/81963/2011.

References

[1] J.-J. Brière, D. Schlemmer, D. Chretien, P. Rustin, Quinone analogues regulate mitochondrial substrate competitive oxidation, Biochem. Biophys. Res. Commun. 316 (2004) 1138–1142.
[2] M. Floreani, F. Carpenedo, One- and two-electron reduction of menadione in guinea-pig and rat cardiac tissue, Gen. Pharmacol. 23 (1992) 757–762.
[3] U.A. Boelsterli, Mechanistic Toxicology: The Molecular Basis of How Chemicals Disrupt Biological Targets, Second edition CRC Press, Boca Raton, USA, 2003.
[4] L.M. Nutter, C. Ann-Lii, H. Hsiao-Ling, H. Ruey-Kun, E.O. Ngo, L. Tsang-Wu, Menadione: spectrum of anticancer activity and effects on nucleotide metabolism in human neoplastic cell lines, Biochem. Pharmacol. 41 (1991) 1283–1292.
[5] I. Laux, A. Nel, Evidence that oxidative stress-induced apoptosis by menadione involves Fas-dependent and Fas-independent pathways, Clin. Immunol. 101 (2001) 335–344.
[6] S. Matzno, Y. Yamaguchi, T. Akiyoshi, T. Nakabayashi, K. Matsuyama, An attempt to evaluate the effect of vitamin K3 using as an enhancer of anticancer agents, Biol. Pharm. Bull. 31 (2008) 1270–1273.
[7] M. Tetef, K. Margolin, C. Ahn, S. Akman, W. Chow, P. Coluzzi, L. Leong, R.J. Morgan, J. Raschko, S. Shibata, G. Somlo, J.H. Doroshow, Mitomycin C and menadione for the treatment of advanced gastrointestinal cancers: a phase II trial, J. Cancer Res. Clin. Oncol. 121 (1995) 103–106.
[8] M. Tetef, K. Margolin, C. Ahn, S. Akman, W. Chow, L. Leong, R.J. Morgan, J. Raschko, G. Somlo, J.H. Doroshow, Mitomycin C and menadione for the treatment of lung cancer: a phase II trial, Invest. New Drugs 13 (1995) 157–162.
[9] S. Osada, H. Tomita, Y. Tanaka, Y. Tokuyama, H. Tanaka, F. Sakashita, T. Takahashi, The utility of vitamin K3 (menadione) against pancreatic cancer, Anticancer. Res. 28 (2008) 45–50.
[10] J.M. Jamison, J. Gilloteaux, H.S. Taper, J.L. Summers, Evaluation of the in vitro and in vivo antitumor activities of vitamin C and K-3 combinations against human prostate cancer, J. Nutr. 131 (2001) 158S–160S.
[11] O.M. Alarcón, F. Vásquez, A. Acosta, J.L. Burguera, M. Burguera, S.Y. Ortega, Hematologic changes in rats treated with high doses of vitamin K3 (menadione), Arch. Latinoam. Nutr. 41 (1991) 363–374.
[12] R. Munday, B.L. Smith, E.A. Fowke, Haemolytic activity and nephrotoxicity of 2-hydroxy-1,4-naphthoquinone in rats, J. Appl. Toxicol. 11 (1991) 85–90.
[13] W.F. Tzeng, T.J. Chiou, J.Y. Huang, Y.H. Chen, Menadione-induced cardiotoxicity is associated with alteration in intracellular Ca2+ homeostasis, Proc. Natl. Sci. Counc. Repub. China B 16 (1992) 84–90.
[14] S.-P. Ip, H.-Y. Yiu, K.-M. Ko, Schisandrin B protects against menadione-induced hepatotoxicity by enhancing DT-diaphorase activity, Mol. Cell. Biochem. 208 (2000) 151–155.
[15] E.J. White, J.B. Clark, Menadione-treated synaptosomes as a model for post-ischaemic neuronal damage, Biochem. J. 253 (1988) 425–433.
[16] C. Luxo, A.S. Jurado, J.B.A. Custódio, V.M. Madeira, Use of *Bacillus stearothermophilus* as a model to study tamoxifen-membrane interactions, Toxicol. Vitro 10 (1996) 463–471.
[17] J.P. Monteiro, J.D. Martins, P.C. Luxo, A.S. Jurado, V.M.C. Madeira, Molecular mechanisms of the metabolite 4-hydroxytamoxifen of the anticancer drug tamoxifen: use of a model microorganism, Toxicol. Vitro 17 (2003) 629–634.
[18] C. Sousa, C. Nunes, M. Lúcio, H. Ferreira, J.L.F.C. Lima, J. Tavares, A. Cordeiro-da-Silva, S. Reis, Effect of nonsteroidal anti-inflammatory drugs on the cellular membrane fluidity, J. Pharm. Sci. 97 (2008) 3195–3206.
[19] J.P. Monteiro, A.F. Martins, M. Lúcio, S. Reis, T.J.T. Pinheiro, C.F.G.C. Geraldes, P.J. Oliveira, A.S. Jurado, Nimesulide interaction with membrane model systems: are membrane physical effects involved in nimesulide mitochondrial toxicity? Toxicol. Vitro 25 (2011) 1215–1223.
[20] M.M. Donato, A.S. Jurado, M.C. Antunes-Madeira, V.M.C. Madeira, *Bacillus stearothermophilus* as a model to evaluate membrane toxicity of a lipophilic environmental pollutant (DDT), Arch. Environ. Contam. Toxicol. 33 (1997) 109–116.
[21] J.D. Martins, J.P. Monteiro, M.C. Antunes-Madeira, A.S. Jurado, V.M.C. Madeira, Use of the microorganism *Bacillus stearothermophilus* as a model to evaluate toxicity of the lipophilic environmental pollutant endosulfan, Toxicol. Vitro 17 (2003) 595–601.
[22] J. Monteiro, R. Videira, M. Matos, A. Dinis, A. Jurado, Non-selective toxicological effects of the insect juvenile hormone analogue methoprene. A membrane biophysical approach, Appl. Biochem. Biotechnol. 150 (2008) 243–257.
[23] C. Nunes, C. Sousa, H. Ferreira, M. Lucio, J.L. Lima, J. Tavares, A. Cordeiro-da-Silva, S. Reis, Substituted phenols as pollutants that affect membrane fluidity, J. Environ. Biol. 29 (2008) 733–738.
[24] J.D. Martins, A.S. Jurado, A.J.M. Moreno, V.M.C. Madeira, Comparative study of tributyltin toxicity on two bacteria of the genus *Bacillus*, Toxicol. Vitro 19 (2005) 943–949.
[25] H.G. Shertzer, L. Låstbom, M. Sainsbury, P. Moldéus, Menadione-mediated membrane fluidity alterations and oxidative damage in rat hepatocytes, Biochem. Pharmacol. 43 (1992) 2135–2141.
[26] P.-C. Klöhn, H.-G. Neumann, Impairment of respiration and oxidative phosphorylation by redox cyclers 2-nitrosofluorene and menadione, Chem. Biol. Interact. 106 (1997) 15–28.
[27] P.A. Janmey, P.K.J. Kinnunen, Biophysical properties of lipids and dynamic membranes, Trends Cell Biol. 16 (2006) 538–546.

[28] W. De Vrij, R.A. Bulthuis, K.W.N., Comparative study of energy-transducing properties of cytoplasmic membranes from mesophilic and thermophilic *Bacillus* species, J. Bacteriol. 170 (1988) 2359–2366.
[29] L. Yang, L. Ding, H.W. Huang, New phases of phospholipids and implications to the membrane fusion problem, Biochemistry 42 (2003) 6631–6635.
[30] P.V. Escribá, Membrane-lipid therapy: a new approach in molecular medicine, Trends Mol. Med. 12 (2006) 34–43.
[31] O. Vogler, J. Casas, D. Capó, T. Nagy, G. Borchert, G. Martorell, P.V. Escribá, The Gbetagamma dimer drives the interaction of heterotrimeric Gi proteins with nonlamellar membrane structures, J. Biol. Chem. 279 (2004) 36540–36545.
[32] F. Gonzalvez, E. Gottlieb, Cardiolipin: setting the beat of apoptosis, Apoptosis 12 (2007) 877–885.
[33] J.V. Gerasimenko, O.V. Gerasimenko, A. Palejwala, A.V. Tepikin, O.H. Petersen, A.J.M. Watson, Menadione-induced apoptosis: roles of cytosolic Ca2 + elevations and the mitochondrial permeability transition pore, J. Cell Sci. 115 (2002) 485–497.
[34] A. Toninello, M. Salvi, M. Schweizer, C. Richter, Menadione induces a low conductance state of the mitochondrial inner membrane sensitive to bongkrekic acid, Free Radic. Biol. Med. 37 (2004) 1073–1080.
[35] A.G. Kruglov, K.B. Subbotina, N.-E.L. Saris, Redox-cycling compounds can cause the permeabilization of mitochondrial membranes by mechanisms other than ROS production, Free Radic. Biol. Med. 44 (2008) 646–656.
[36] P. Gazotti, K. Malmstrom, M. Crompton, Membrane Biochemistry. A Laboratory Manual on Transport and Bioenergetics, Springer-Verlag, New York, 1979, pp. 62–69.
[37] A.G. Gornall, C.J. Bardawill, M.M. David, Determination of serum proteins by means of the biuret reaction, J. Biol. Chem. 177 (1949) 751–766.
[38] J.G. Satav, S.S. Katyare, P. Fatterpaker, A. Sreenivasan, Further characterization of rat liver mitochondrial fractions. Lipid composition and synthesis, and protein profiles, Biochem. J. 156 (1976) 215–223.
[39] L.M. Magalhaes, C. Nunes, M. Lucio, M.A. Segundo, S. Reis, J.L. Lima, High-throughput microplate assay for the determination of drug partition coefficients, Nat. Protoc. 5 (2010) 1823–1830.
[40] J.R. Lakowicz, Principles of Fluorescence Spectroscopy, 3rd edition Springer, New York, 2006.
[41] G.R. Bartlett, Phosphorus assay in column chromatography, J. Biol. Chem. 234 (1959) 466–468.
[42] C.J.F. Bottcher, C.M. van Gent, C. Pries, A rapid and sensitive sub-micro phosphorus determination, Anal. Chim. Acta 24 (1961) 203–204.
[43] J.A. Monti, S.T. Christian, W.A. Shaw, Synthesis and properties of a highly fluorescent derivative of phosphatidylethanolamine, J. Lipid Res. 19 (1978) 222–228.
[44] R.F. Epand, M.A. Schmitt, S.H. Gellman, R.M. Epand, Role of membrane lipids in the mechanism of bacterial species selective toxicity by two [alpha]/[beta]-antimicrobial peptides, Biochim. Biophys. Acta Biomembr. 1758 (2006) 1343–1350.
[45] P.R. Cullis, B. de Kruijff, Lipid polymorphism and the functional roles of lipids in biological membranes, Biochim. Biophys. Acta 559 (1979) 399–420.
[46] R.P. Rand, S. Sengupta, Cardiolipin forms hexagonal structures with divalent cations, Biochim. Biophys. Acta Biomembr. 255 (1972) 484–492.
[47] M.P. Andrich, J.M. Vanderkooi, Temperature dependence of 1,6-diphenyl-1, 3,5-hexatriene fluorescence in phospholipid artificial membranes, Biochemistry 15 (1976) 1257–1261.
[48] F.G. Prendergast, R.P. Haugland, P.J. Callahan, 1-[4-(Trimethylamino) phenyl]-6-phenylhexa-1,3,5-triene: synthesis, fluorescence properties, and use as a fluorescence probe of lipid bilayers, Biochemistry 20 (1981) 7333–7338.
[49] G. Loor, J. Kondapalli, J.M. Schriewer, N.S. Chandel, T.L. Vanden Hoek, P.T. Schumacker, Menadione triggers cell death through ROS-dependent mechanisms involving PARP activation without requiring apoptosis, Free Radic. Biol. Med. 49 (2010) 1925–1936.
[50] F.R. Heinzel, Y. Luo, X. Li, K. Boengler, A. Buechert, D. Garcia-Dorado, F. Di Lisa, R. Schulz, G. Heusch, Impairment of diazoxide-induced formation of reactive oxygen species and loss of cardioprotection in Connexin 43 deficient mice, Circ. Res. 97 (2005) 583–586.
[51] Y.-Y.E. Chuang, Y. Chen, Gadisetti, V.R. Chandramouli, J.A. Cook, D. Coffin, M.-H. Tsai, W. DeGraff, H. Yan, S. Zhao, A. Russo, E.T. Liu, J.B. Mitchell, Gene expression after treatment with hydrogen peroxide, menadione, or t-butyl hydroperoxide in breast cancer cells, Cancer Res. 62 (2002) 6246–6254.
[52] X. Luo, S. Pitkanen, S. Kassovska-Bratinova, B.H. Robinson, D.C. Lehotay, Excessive formation of hydroxyl radicals and aldehydic lipid peroxidation products in cultured skin fibroblasts from patients with complex I deficiency, J. Clin. Invest. 99 (1997) 2877–2882.
[53] H. Sakagami, K. Satoh, Y. Hakeda, M. Kumegawa, Apoptosis-inducing activity of vitamin C and vitamin K, Cell. Mol. Biol. 46 (2000) 129–143.
[54] V. Grishko, M. Solomon, G.L. Wilson, S.P. LeDoux, M.N. Gillespie, Oxygen radical-induced mitochondrial DNA damage and repair in pulmonary vascular endothelial cell phenotypes, Am. J. Physiol. Lung Cell Mol. Physiol. 280 (2001) L1300–L1308.
[55] J.A. Woods, A.J. Young, I.T. Gilmore, A. Morris, R.F. Bilton, Measurement of menadione-mediated DNA damage in human lymphocytes using the comet assay, Free Radic. Res. 26 (1997) 113–124.
[56] T.J. Chiou, Y.T. Chou, W.F. Tzeng, Menadione-induced cell degeneration is related to lipid peroxidation in human cancer cells, Proc. Natl. Sci. Counc. Repub. China B 22 (1998) 13–21.
[57] J.H. Ipsen, K. Jorgensen, O.G. Mouritsen, Density fluctuations in saturated phospholipid bilayers increase as the acyl-chain length decreases, Biophys. J. 58 (1990) 1099–1107.
[58] D.N. Criddle, J.V. Gerasimenko, H.K. Baumgartner, M. Jaffar, S. Voronina, R. Sutton, O.H. Petersen, O.V. Gerasimenko, Calcium signalling and pancreatic cell death: apoptosis or necrosis? Cell Death Differ. 14 (2007) 1285–1294.
[59] D. Ardail, J.P. Privat, M. Egret-Charlier, C. Levrat, F. Lerme, P. Louisot, Mitochondrial contact sites. Lipid composition and dynamics, J. Biol. Chem. 265 (1990) 18797–18802.
[60] M. Crompton, The mitochondrial permeability transition pore and its role in cell death, Biochem. J. 341 (1999) 233–249.